Electronic Supplementary Information (ESI) for

Low-Molecular-Weight Supramolecular Adhesives based on Non-covalent Self-assembly of Small Molecular Gelator

Yujia Liang,[a,†] Kaifang Wang,[a,†] Jingjing Li*[b], Yunfei Zhang,[a] Junpeng Liu,[a] Kaihuang Zhang,[a] Yihan Cui,[a] Mengke Wang,[a] and Chun-Sen Liu*[a]

[a] Henan Provincial Key Laboratory of Surface & Interface Science, Zhengzhou University of Light Industry, Zhengzhou 450002, China. E-mail: chunsenliu@zzuli.edu.cn.

[b] School of Chemistry and Chemical Engineering, Henan University of Technology, Zhengzhou, 450001, China. E-mail: nicoleljj@tju.edu.cn.

† These authors contributed equally to this work.

Table of Contents

Video S1

Ultra-low temperature (liquid nitrogen, –196 ºC) resistant adhesiveness of C_{12}TAB eutectogel.

Video S2

Underwater *in situ* adhesiveness of C_{12}TAB eutectogel.

Video S3

Comparison of the underwater *in situ* adhesiveness (C_{12}TAB eutectogel *vs* commerical adhesives).

Video S4

Organic solvent *in situ* adhesiveness of C_{12}TAB eutectogel and commerical adhesives.

Video S5

The conformational states of C_{12}TAB eutectogel on glass and PTFE surfaces under a certain acceleration.

Section S1 Methods

1. Materials

Urea (AR, 99%), Choline Chloride (AR, 98%), Chlormequat chloride (AR, 98%), Ethylamine hydrochloride (AR, 98%), and Dodecyl trimethyl ammonium bromide (AR, 99%) were purchased from Tokyo Chemical Industry Company. Hexyl trimethyl ammonium bromide (AR, 98%), Trimethyl octyl ammonium bromide (AR, 98%), Decyl trimethyl ammonium bromide (AR, 99%), Myristyl trimethyl ammonium bromide (AR, 99%), Cetyl trimethyl ammonium bromide (AR, 98%), Trimethyl octadecyl ammonium bromide (AR, 98%), Thiourea (ACS, 99%), 1,3-Dimethylurea (AR, 98%) were purchased from Beijing Innochem Science & Technology Co. Ltd.. Acetamide (AR, 99%) and Tetramethyl ammonium chloride (AR, 99%) were purchased from Acros. All other chemicals used in this work are commercial analytical grade reagents without further purification.

2. Instruments

Powder X-ray diffraction (PXRD) profiles were performed using a Bruker D8 Advance X-ray diffractometer using Cu Kα radiation at 25 ℃. FTIR spectra of the samples were measured by Nicolet 5700 FTIR. Carle Zeiss LSM710 confocal laser scanning microscope, scanning electron microscope (SEM, JSM-7001F) and transmission electron microscope (TEM, JEM 2100) were used to observe the morphology of the eutectogels. Rheological tests were performed by using a Hake Mars rheometer (Thermo Scientific) with a parallel plate geometry (20 mm, 0.5 mm gap). Frequency sweeps were conducted from 0.1 to 100 rad s^{-1} at a fixed strain of 0.1%. Strain sweeps were conducted from 0.1% to 100% at a fixed frequency of 1 Hz. Temperature-dependent rheological tests were conducted at a fixed shear rate of 1 rad s^{-1}. The temperature range of the rotated rheometer was adjusted from 5 to 80 ℃. The lap shear test conducted by a UTM2202 or UTM2503 electronic universal testing machine with a pull rate of 10 mm s^{-1} (at least three parallel samples were used for each measurement). For each test, the adhesion area on the surfaces was about 2.0 cm × 3.0 cm.

3. Preparation of deep eutectic solvents (DESs)

DES was prepared by stirring choline chloride (ChCl) and urea in a mole ratio of 1:2 at 60 ℃ until a homogeneous solution was formed. The obtained DES was referred to as ChCl-urea. Other DESs were prepared following a similar procedure.

4. Preparation of the supramolecular eutectogels

Taking 25.0 wt% dodecyl trimethyl ammonium bromide (C_{12}TAB) supramolecular eutectogel as an example: C_{12}TAB (400.0 mg, 1.3 mmol) was added to a clean vial, followed by addition of 1200.0 mg ChCl-urea DES. The system was heated (~100 ℃) until the solid was totally dissolved, after which the solution was allowed to cool to room temperature. Eutectogel was considered to have formed when no gravitational flow occurred upon inversion of the vial. The gel-sol phase transition temperatures of the eutectogels were tested by falling ball method, and the critical gelator concentration was the lowest concentration that can form a stable gel evaluated by invert tube method. The dried C_{12}TAB/ChCl-urea eutectogels for SEM, FTIR and XRD test were prepared via a solvent-exchange method. Other supramolecular eutectogels were prepared following a similar procedure.

5. Adhesion test

Preparation of adhesive layers in air and dry surface. C_{12}TAB/ChCl-urea supramolecular eutectogel adhesive was prepared following a similar procedure to the bulk material as described above. Briefly, 400.0 mg of C_{12}TAB (1.3 mmol) was completely dissolved into 1200.0 mg ChCl-urea DES upon heating. The obtained homogenous solution before gelation was then pipetted on different substrates including glass, wood and various metal plates, poly(methyl methacrylate) (PMMA) and polytetrafluoroethylene (PTFE). And then another substrate was covered on the coating layer. After pressing for ~2 min in air at room temperature, the two plates adhered immediately and firmly together. The adhered plates were further used for lap-shear test. For each test, the adhesion area on the surfaces was about 2.0 cm × 3.0 cm, the volume of the adhesive was about 0.1 mL, and thickness of the adhesive between substrates was about 0.17 mm. The pressing load was about 3 kPa. Other adhesive layers were also prepared following a similar procedure.

Underwater, organic solvents and low temperature adhesion test. The preparation of the adhesive layers was similar as described above, but the whole process was carried out in the presense of water, organic solvents or at low temperatures. The low temperature environment (from 0 ℃ to −80 ℃) was controled via a ultra-low temperature freezer (MeLing company, China).

Ultra-low temperature resistant adhesion tests. The fabrication of the adhesive layers was the same as the solvent-free process. For ultra-low temperature resistant adhesion at −196 ℃, the plates were adhered at room temperature , then totally immersed in liquid nitrogen (–196 ℃) for more than 1 h before testing (See Video S1). The adhesion strength was immediately tested after the sample was taken out.

6. Computational simulation

Simulation of C_{12}TAB/ChCl-urea eutectogel. The geometric optimization of urea, choline and C_{12}TAB molecules was calculated using Gaussian 16 program[1] in the gas phase by a density functional theory (DFT) method on the B3LYP/6-31G(d) level.[2] The atomic charges of the molecules were calculated by electrostatic surface potential fits, using the Multiwfn program,[3] to obtain restrained electrostatic potential (RESP) charge[4] at the same level.

Molecular dynamics (MD) simulations were conducted using the Gromacs 2020.4 package[5] with GAFF force field.[6] A periodic solvent box was built for the mixture of urea, choline, and C_{12}TAB using Packmol.[7] 4000 urea molecule, 2000 choline and chloride ion, and 720 C_{12}TAB and bromide ion were added to the box to reproduce the experimental molar fractions of the gel mixture. The concentration of C_{12}TAB in the simulation were set to around 400 mg mL^{-1}, which is consistent with the experimental system (25.0 wt%). For C_{12}TAB water solution, 720 C_{12}TAB and bromide ion were added to the box and then filled with water using SPC/E model. After energy minimization of the box, a 1ns MD simulation was carried out in the NPT ensemble to equilibrate the system at a constant pressure of 1 bar and 298 K, coupled to a velocity-rescale thermostat[8] and Berendsen barostat.[9] To obtain the global minimum configuration, two cycles of annealing were carried out at 298 to 800 K in NPT ensemble. During the annealing process, the structure was further relaxed to obtain a steady state with a local energy minimum. Then the box was simulated for 2.5 ns to obtain equilibrated C_{12}TAB/ChCl-urea eutectogel in an NPT

ensemble at 293 K and 1 bar, where the temperature and pressure were controlled by velocity-rescale and Parrinello–Rahman algorithms.[10] The time step of the simulation is 2 fs. Non-bonded interactions were calculated up to a cut-off of 1.0 nm. The particle mesh Ewald method[11] was used for treating long-range electrostatic interactions.

Simulation of the interaction of C_{12}TAB/ChCl-urea eutectogels with SiO_2 and PTFE substrate. In order to further study the interaction mechanisms between C_{12}TAB/ChCl-urea eutectogels and different substrates, MD simulation was performed to obtain the interaction configuration and calculate interaction energy. In this work, a periodic box of C_{12}TAB/ChCl-urea eutectogel and substrate was built using Packmol program.[7] For glass substrate, 1660 urea molecule, 830 choline and chloride ion, 300 C_{12}TAB and bromide ion (corresponding to the concentration of 400 mg mL^{-1}) and a 98.3 × 68.1 × 16.2 nm^3 SiO_2 substrate were added to the box to build the adhesion model. For PTFE, SiO_2 was replaced with a PTFE substrate modeling by 100 tetrafluoroethylene polymer.

MD simulations were conducted using the Gromacs 2020.4 package[5] with GAFF force field[6] for urea, choline, C_{12}TAB and PTFE, and charmm27[12] force field for SiO_2 substrate with parameters provided by previous work.[13] After energy minimization of the box, 500ps MD simulation was carried out in the NPT ensemble to equilibrate the system at a constant pressure of 1 bar and 298 K, coupled to a velocity-rescale thermostat[8] and Berendsen barostat.[9] Afterwards, two cycles of annealing were carried out at 298 to 800 K in NPT ensemble for SiO_2 substrate system. For PTFE substrate system, the annealing was from 298 to 600 K to maintain the stability of the system. Finally, 2.5 ns NPT simulation was performed to get the equilibrated adhesion configuration. The time step of the simulation is 1.0 fs.

To calculate the interaction energy between C_{12}TAB/ChCl-urea eutectogels and different substrate, we reran the trajectory generated in 2.5 ns NPT simulation where the non-bonded interactions and electrostatic interactions were all calculated up to a cut-off of 3.0 nm. The interaction energy was defined as the sum of non-bonded and electrostatic interaction energy.

Section S2 Characterization of C_nTAB eutectogels

Table S1. The gelation properties of C_nTAB in ChCl-urea DES.

C_nTAB	Gelation behaviors[a]	T_{gels} (℃)[b]	CGCs (wt%)[c]
C_6TAB	OG	55.3	22.5
C_8TAB	OG	43.2	2.1
$C_{10}TAB$	OG	48.7	0.2
$C_{12}TAB$	OG	52.2	0.2
$C_{14}TAB$	OG	67.4	0.2
$C_{16}TAB$	OG	65.7	0.2
$C_{18}TAB$	OG	60.3	2.9

a: Gelation behaviors were evaluated by inverted tube method at the concentration of 3.0 wt% except for C_6TAB, which was evaluated at 25.0 wt%. OG = opaque gel. b: the gel-to-sol phase transition temperatures (T_{gels}, ℃) were determined by using the "falling-ball method" at the concentration of 3.0 wt% except for C_6TAB, which was evaluated at 25.0 wt%. c: the critical gelator concentrations (CGCs) were recoreded as the minium concentration of C_nTAB that needed to form a stable eutectogel.

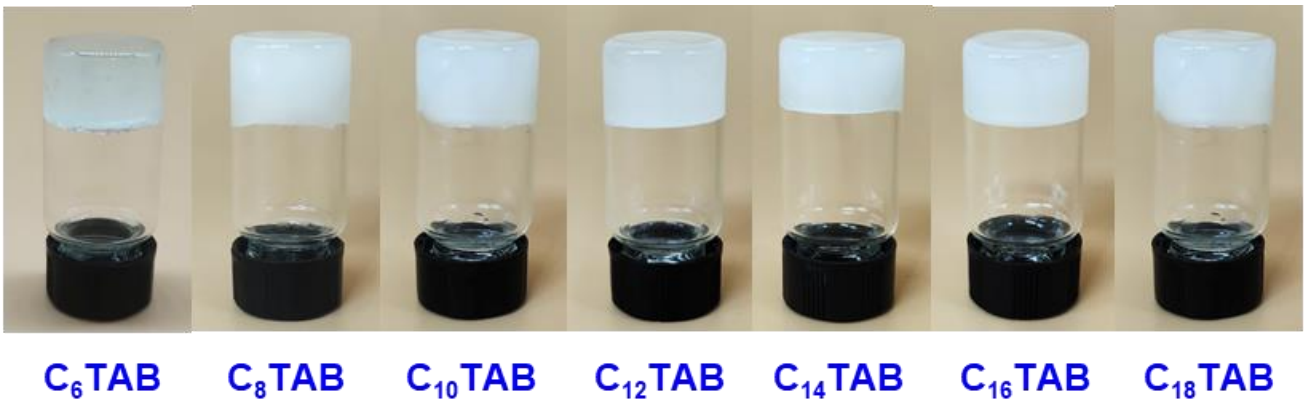

Figure S1. Gelation behaviors of C_nTAB in ChCl-urea DES. The concentration was 25.0 wt% for C_6TAB, and 3.0 wt% for others.

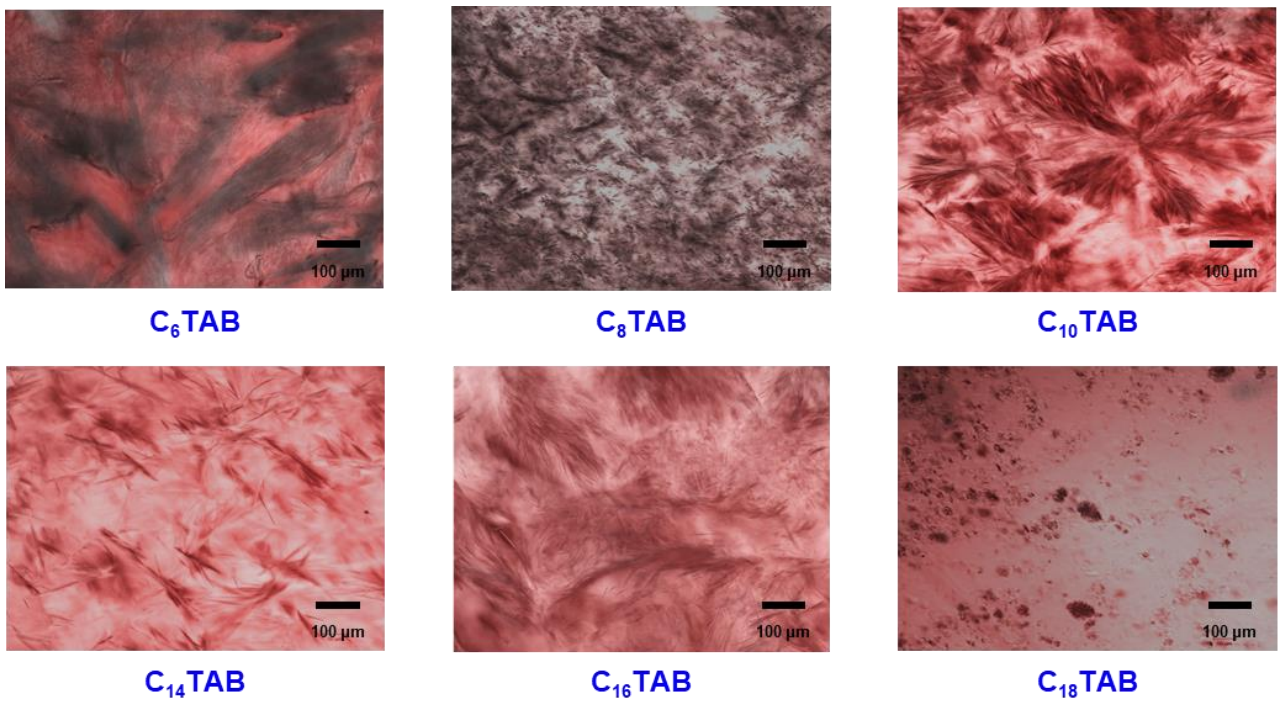

Figure S2. CLSM images of C_nTAB eutectogels in ChCl-urea DES. The concentration was 25.0 wt% for C_6TAB, and 3.0 wt% for others. The eutectogels were labeled with fluoresce in rhodamine B, a red fluorescence probe.

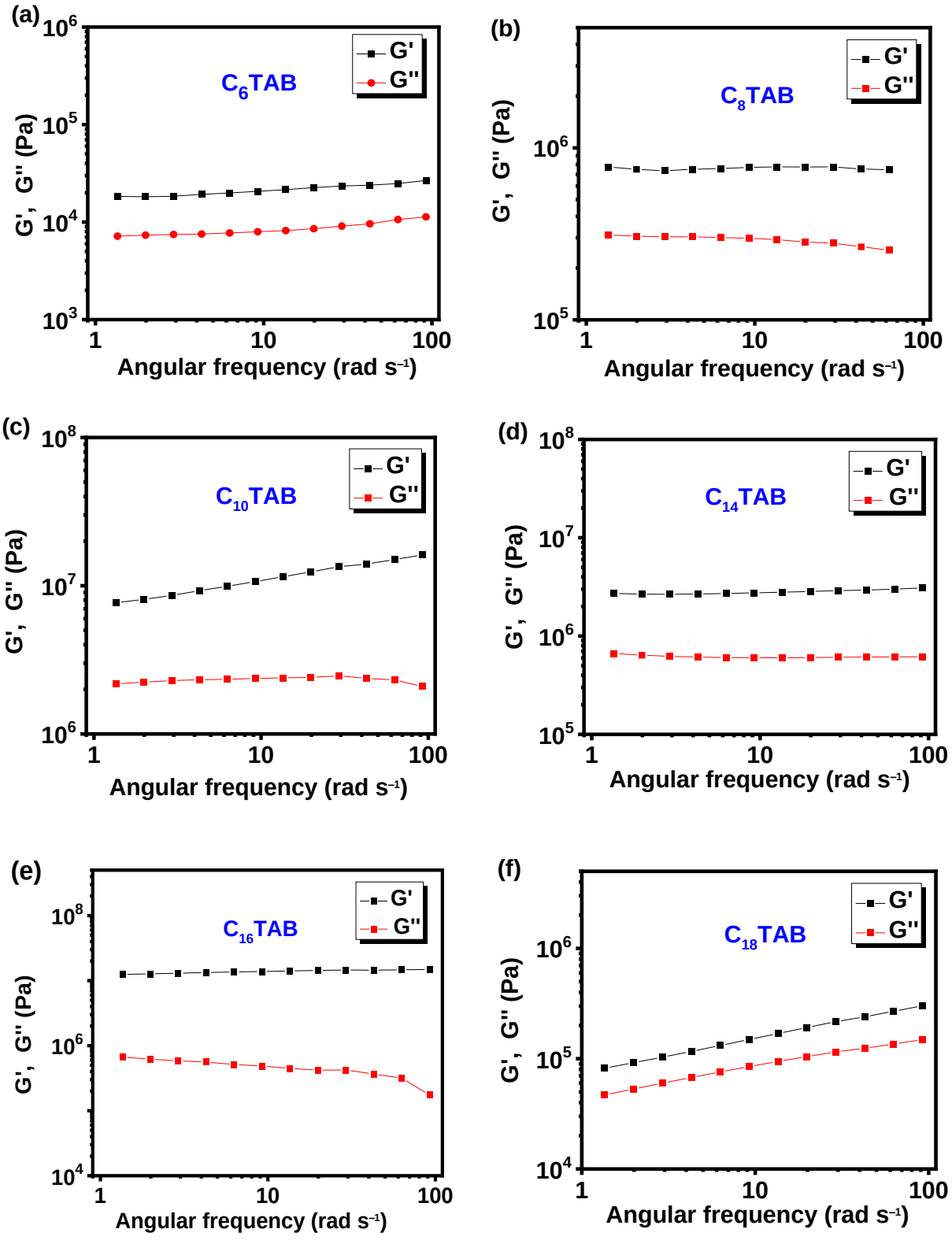

Figure S3. Dynamic frequency sweep of 25.0 wt% C_nTAB/ChCl-urea eutectogels (n = 6, 8, 10, 14, 16, 18) at strain of 0.1%.

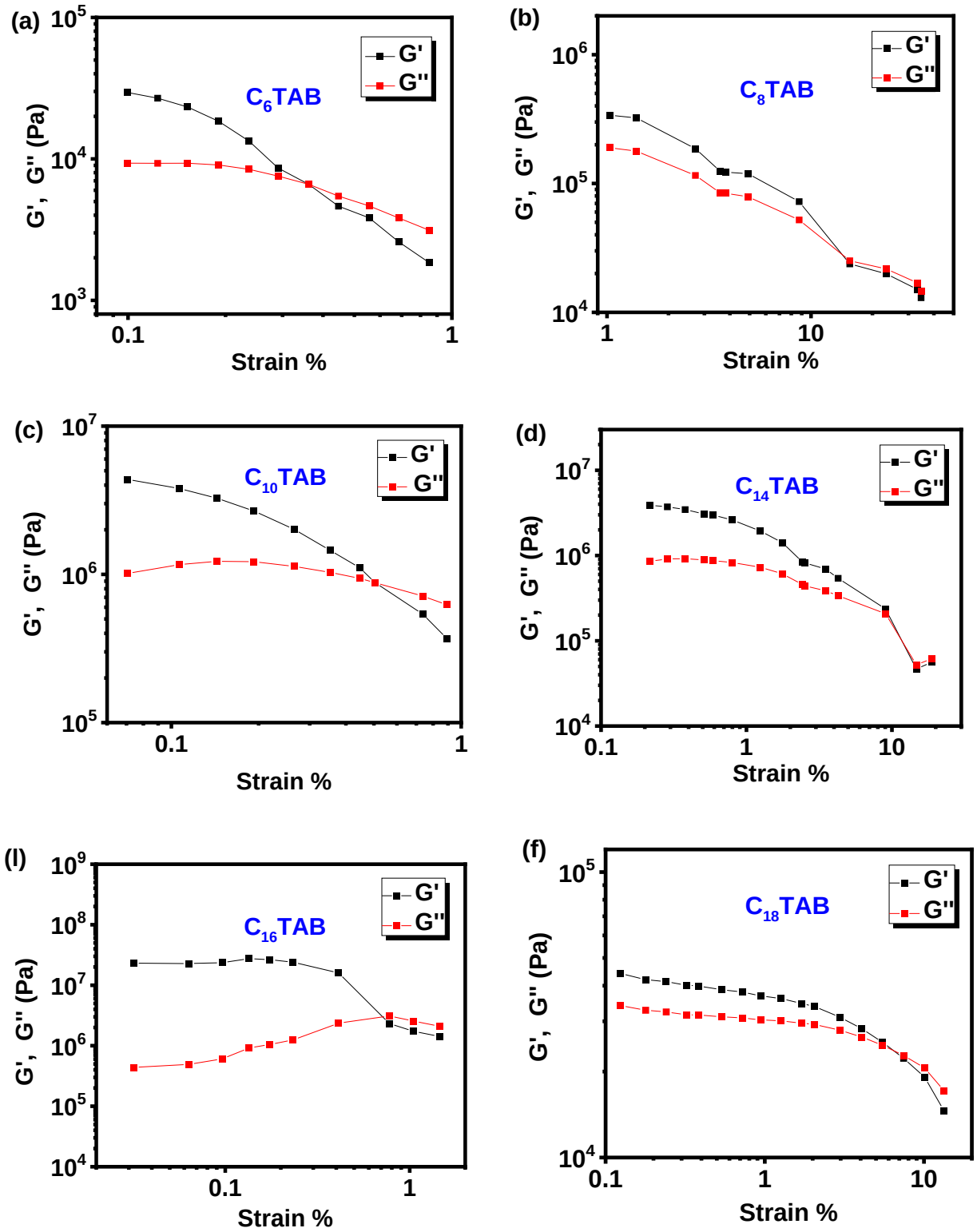

Figure S4. Dynamic strain sweep of 25.0 wt% C_nTAB/ChCl-urea eutectogels (n = 6, 8, 10, 14, 16, 18) at frequency of 1 Hz.

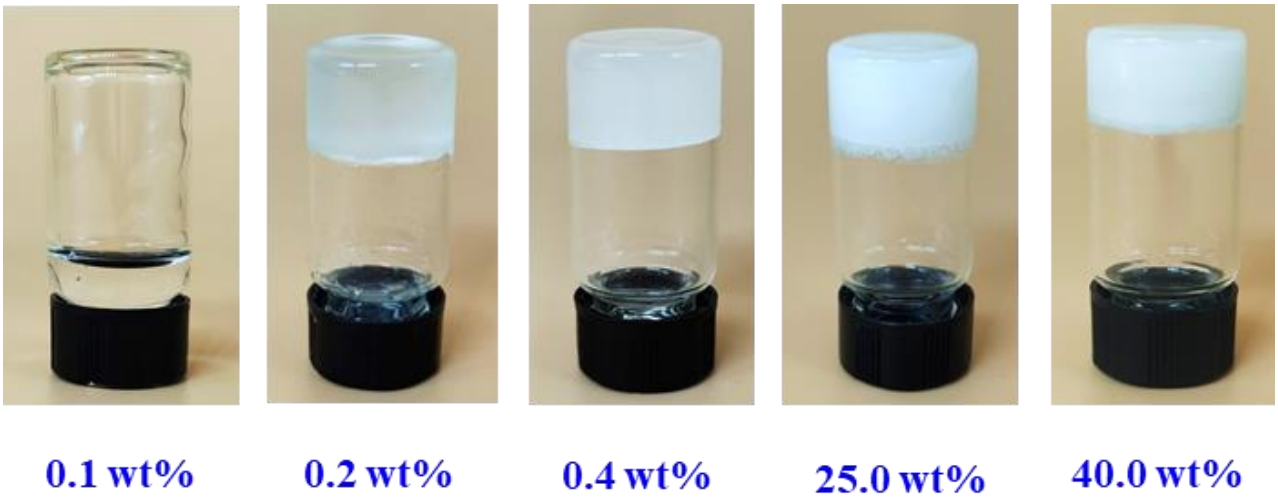

Figure S5. Appearance of C_{12}TAB in ChCl-urea DES at different concentrations.

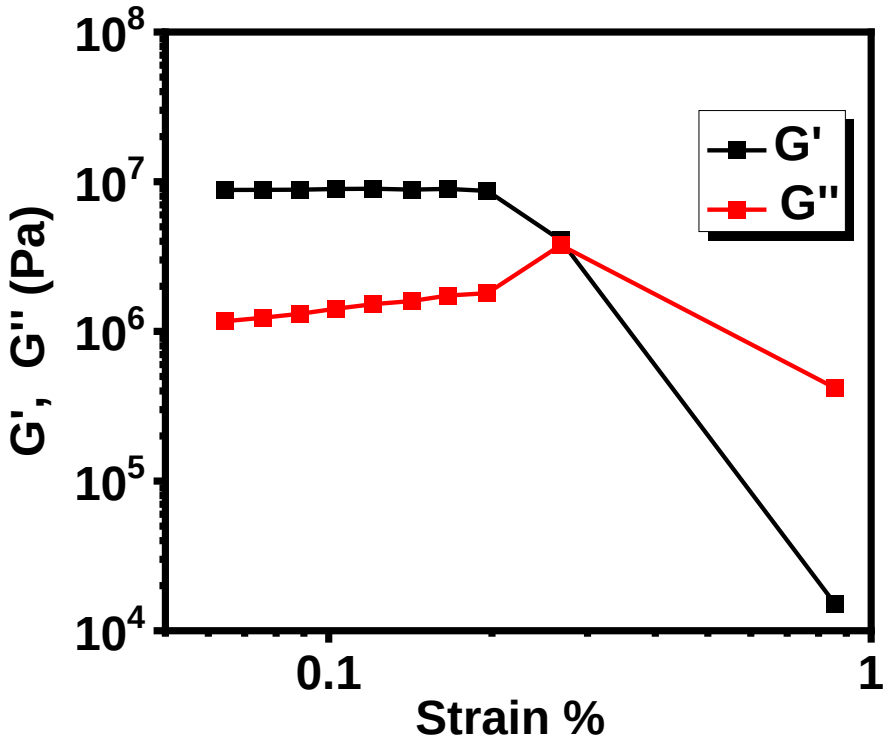

Figure S6. Dynamic strain sweep of 25.0 wt% C_{12}TAB/ChCl-urea eutectogels at frequency of 1 Hz.

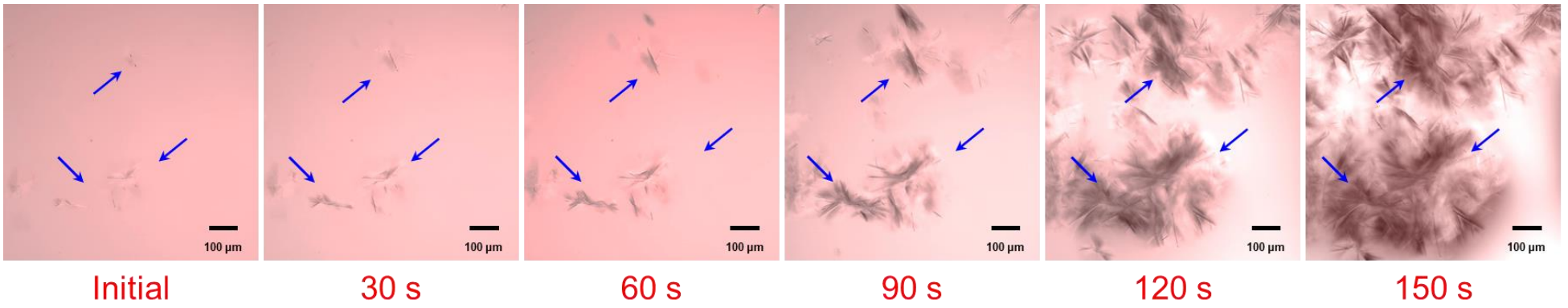

Figure S7. Time-lapse CLSM images of 2.0 wt% C_{12}TAB/ChCl-urea supramolecular eutectogel under different time intervals. The eutectogel was labeled with fluoresce in rhodamine B, a red fluorescence probe.

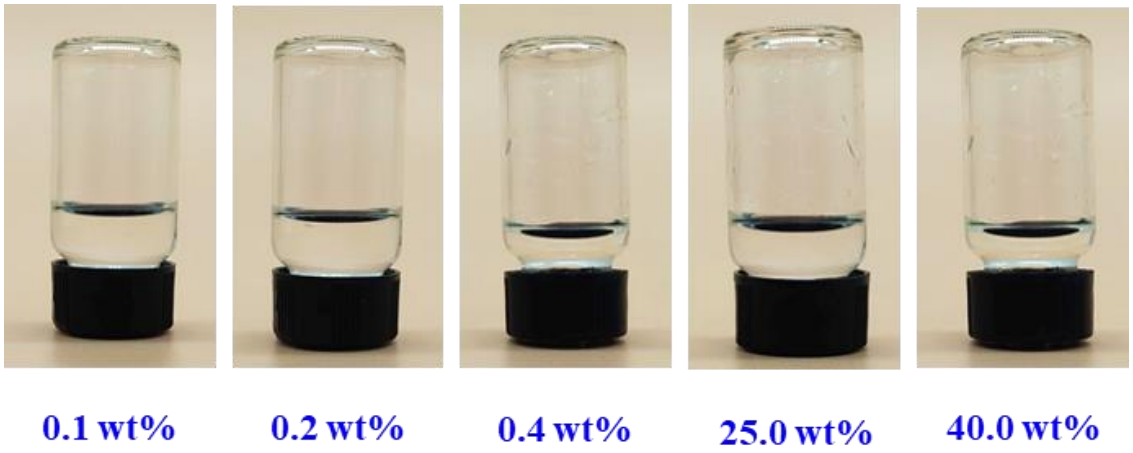

Figure S8. Appearance of C_{12}TAB in water at different concentrations.

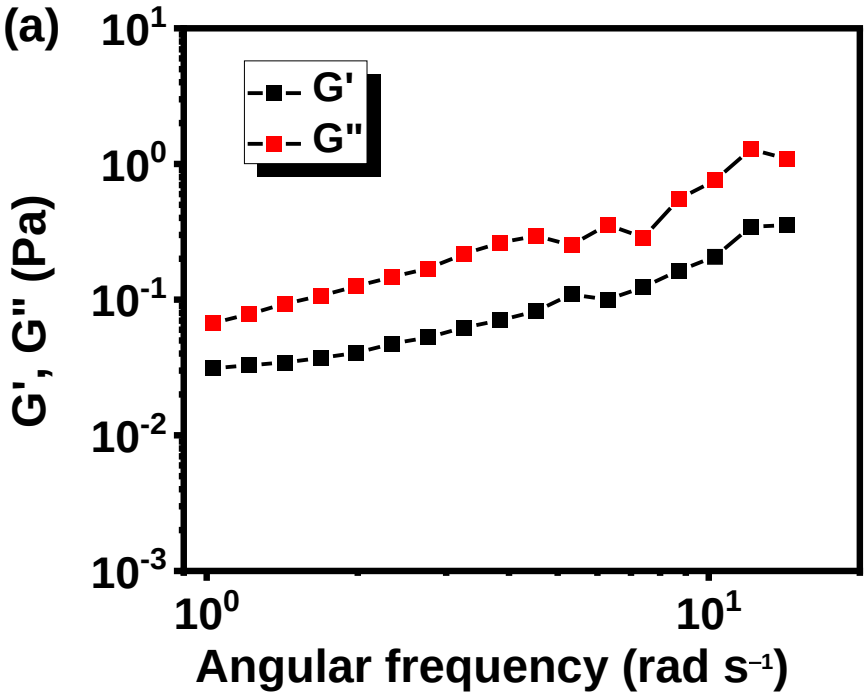

Figure S9. Dynamic frequency sweep of 25.0 wt% C_{12}TAB in water at strain of 0.1%.

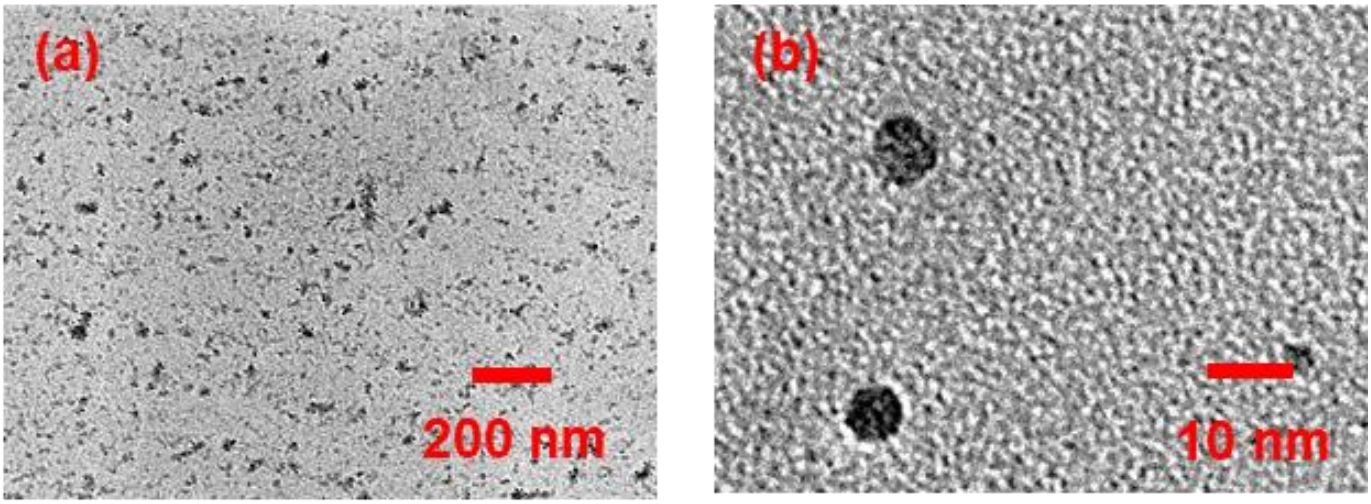

Figure S10. TEM image of lyophilized C_{12}TAB sample in water (2.0 wt%).

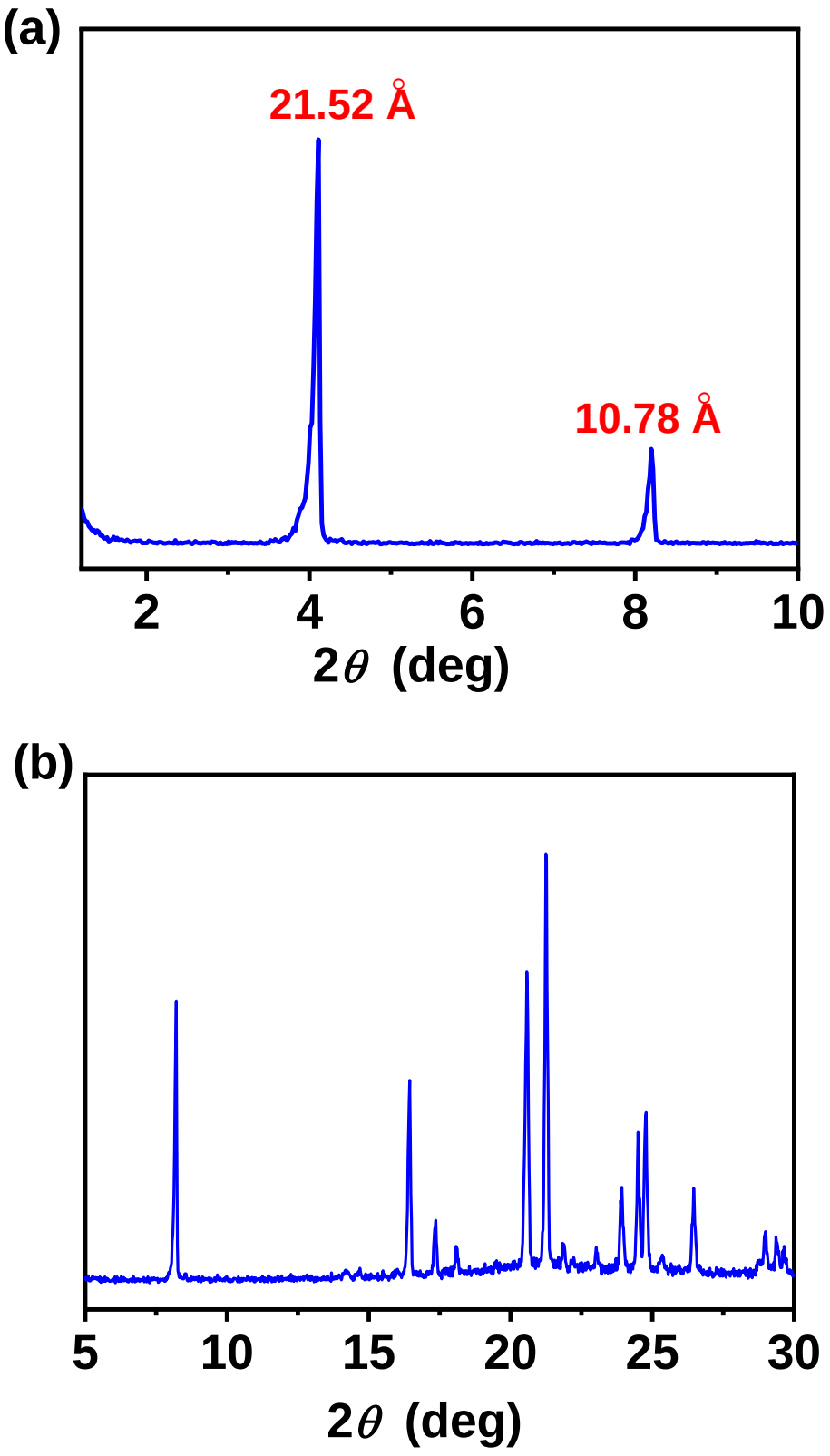

Figure S11. The (a) small-angle and (b) wide-angle XRD patterns of lyophilized C_{12}TAB sample in water (3.0 wt%).

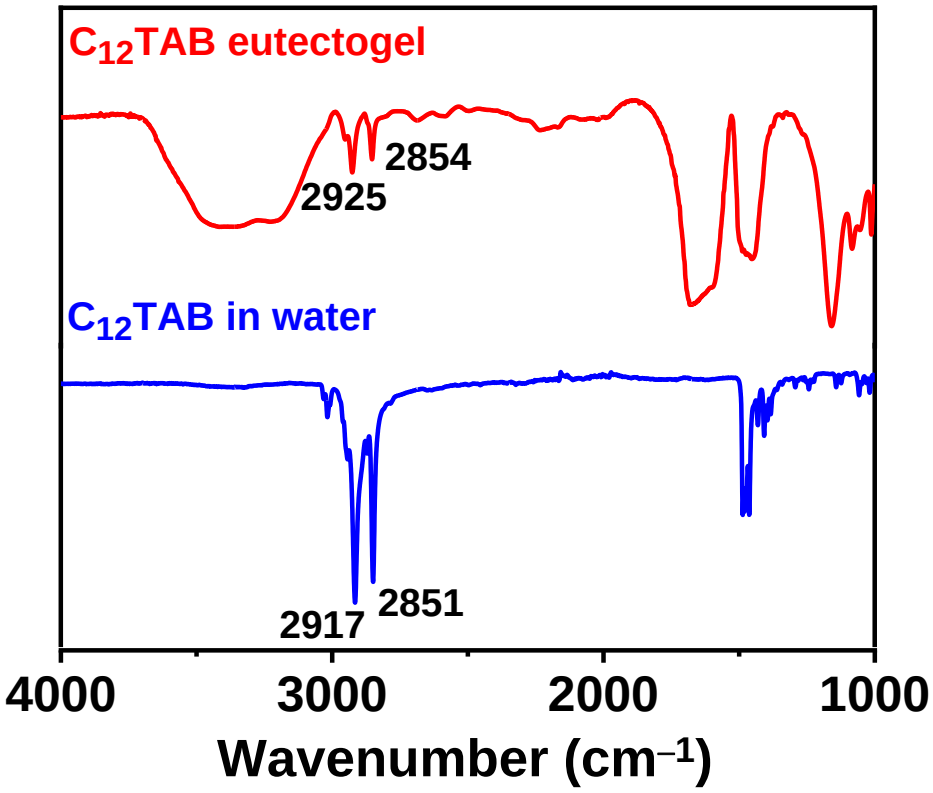

Figure S12. The FT-IR spectra of 3.0 wt% lyophilized C_{12}TAB sample in water and dried C_{12}TAB/ChCl-urea eutectogel.

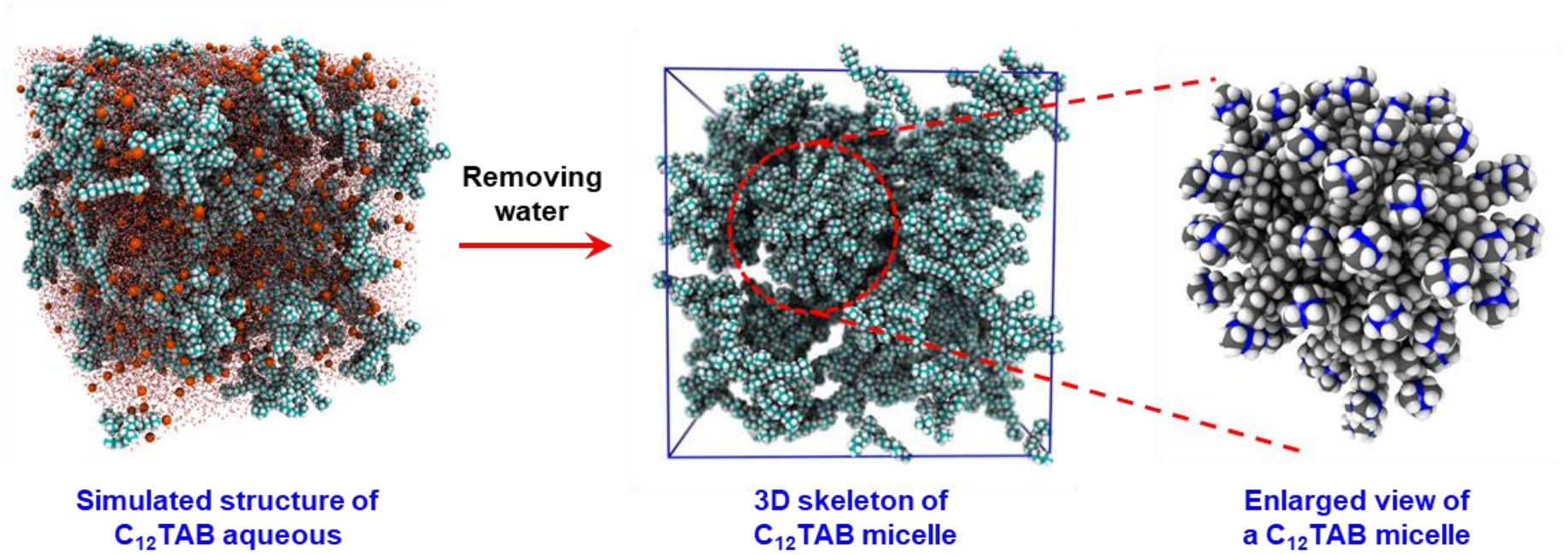

Figure S13. Simulated self-assembly structures of 25.0 wt% C_{12}TAB in water.

Section S3 Adhesion performance of C_nTAB eutectogels

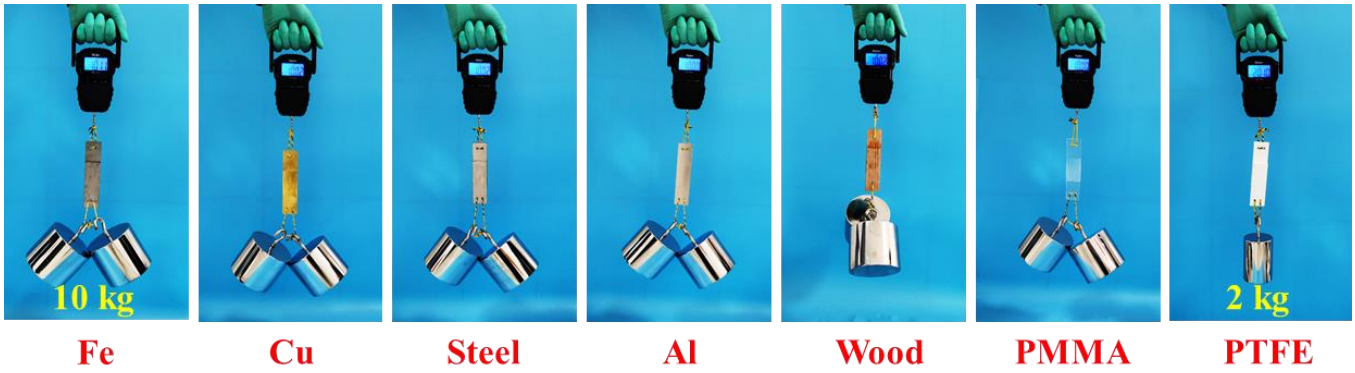

Figure S14. Loading test of 25.0 wt% C_{12}TAB/ChCl-urea eutectogel adhesive to various substrates.

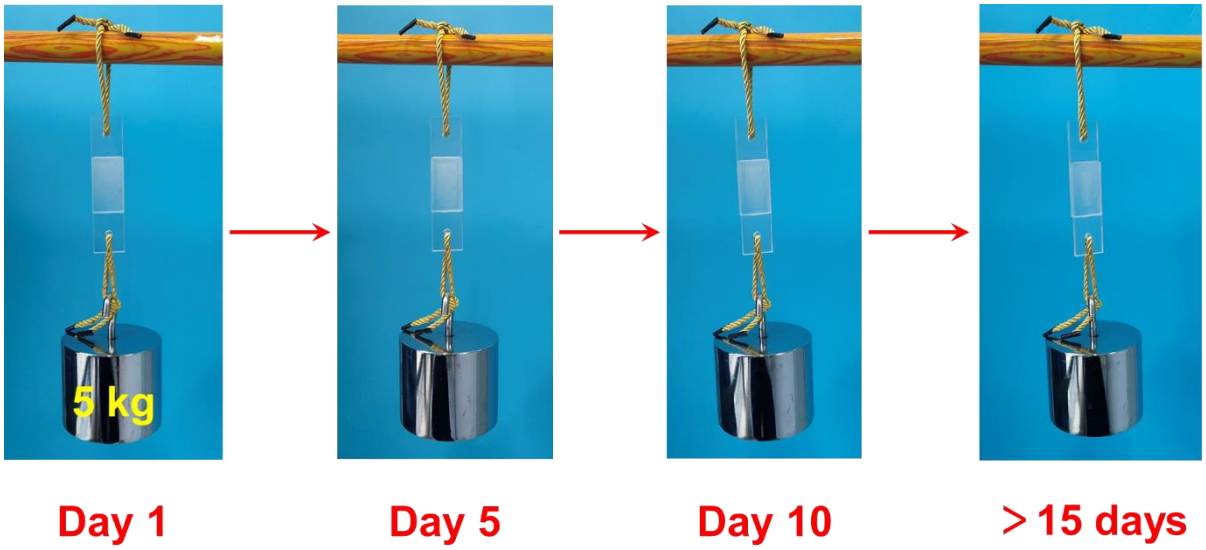

Figure S15. Loading test of long-lasting adhesiveness of 25.0 wt% C_{12}TAB/ChCl-urea eutectogel adhered glass (adhesion area: 3.0 cm × 5.0 cm). The weight (5 kg) was suspended over 15 days without detaching.

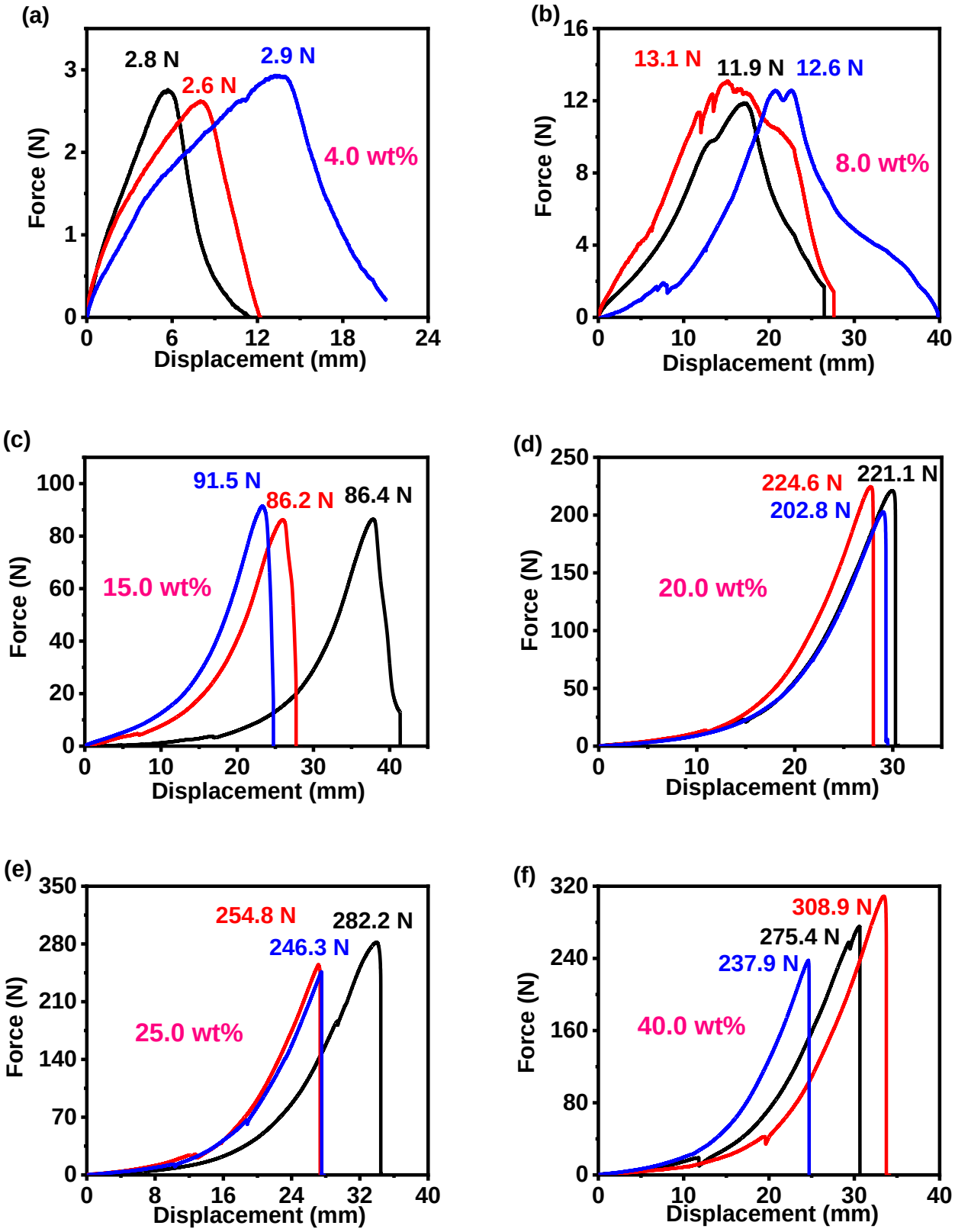

Figure S16. The lap shear test curves of different concentrations of C_{12}TAB/ChCl-urea eutectogel adhered glass (adhesion area: 2.0 cm × 3.0 cm). Data was collected from at least three separate samples.

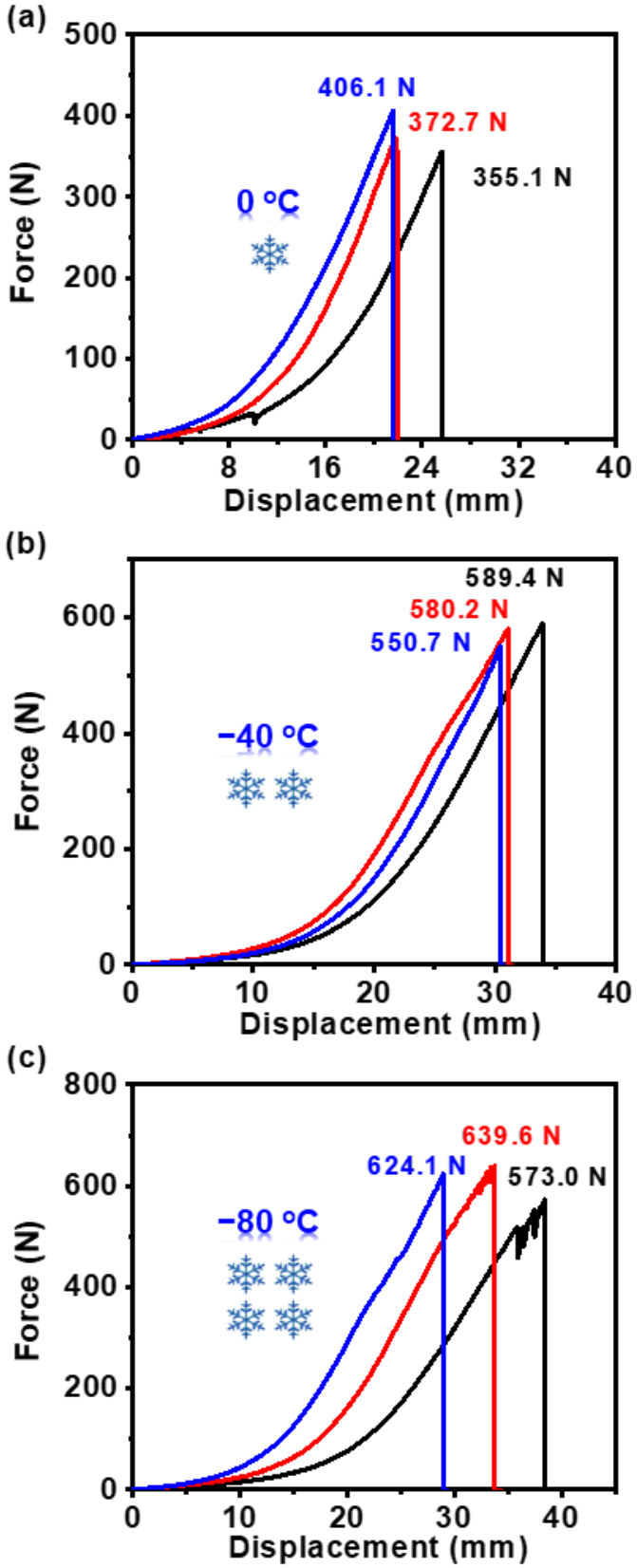

Figure S17. The lap shear test curves of 25.0 wt% C_{12}TAB/ChCl-urea eutectogel adhered glass at different temperatures (adhesion area: 2.0 cm × 3.0 cm). Data was collected from at least three separate samples.

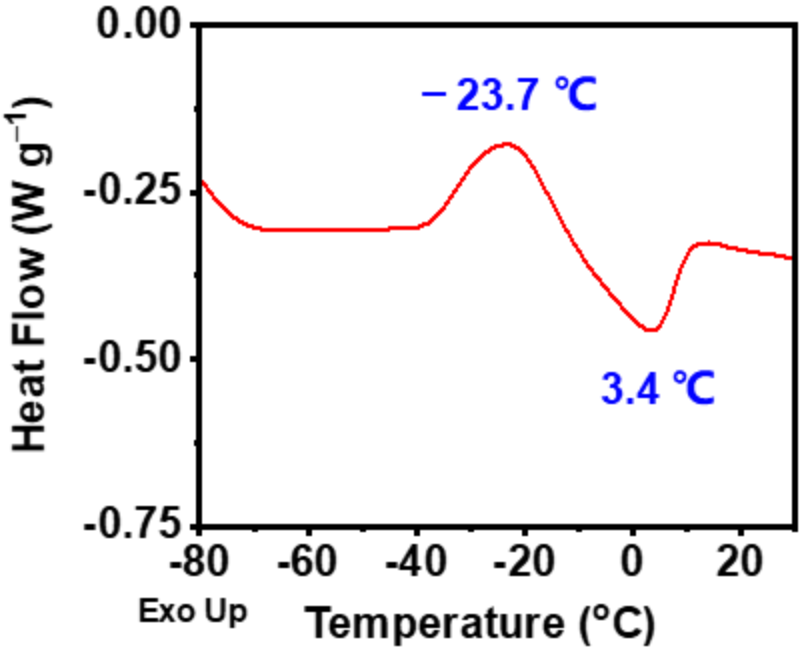

Figure S18. DSC curve of 3.0 wt% C_{12}TAB/ChCl-urea eutectogel.

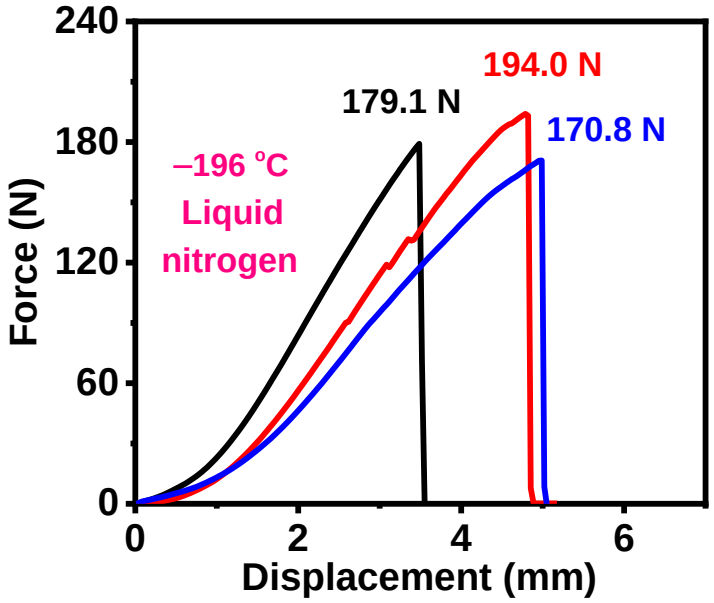

Figure S19. Lap-shear test curve of 25.0 wt% C_{12}TAB/ChCl-urea eutectogel adhered glass after being immersed in immersed in liquid nitrogen (–196 ℃) for over 1 h (adhesion area: 2.0 cm × 3.0 cm). Data was collected from at least three separate samples.

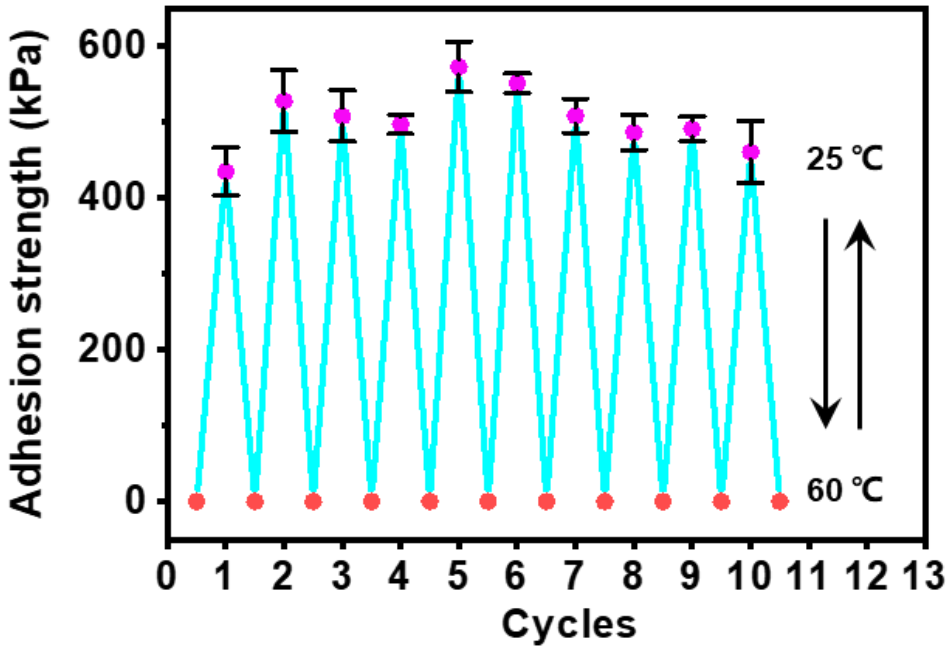

Figure S20. The adhesion strength of the eutectogel after 10 times cycling experiments between 25 and 60 ℃

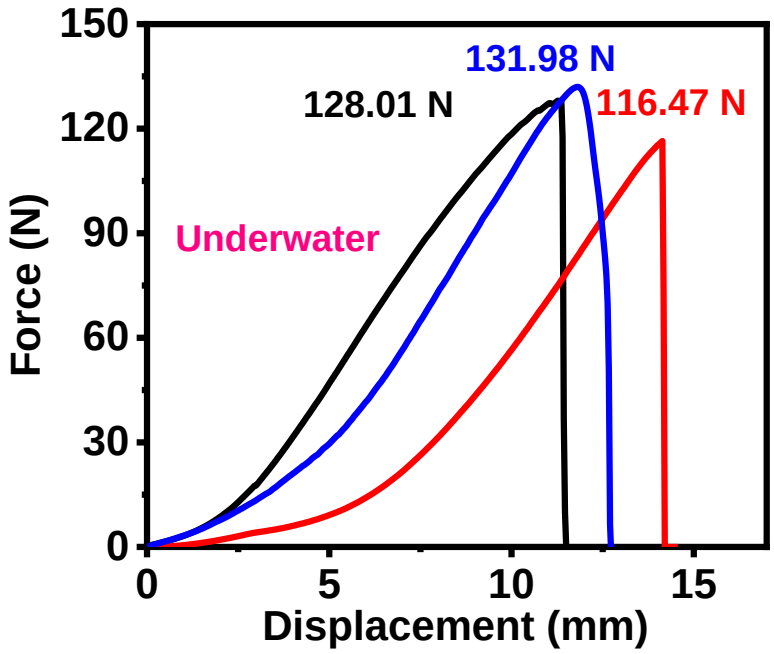

Figure S21. Lap-shear test curve of 25.0 wt% C_{12}TAB/ChCl-urea eutectogel adhered glass. The samples were *in situ* prepared underwater by pressing ~5 min (adhesion area: 2.0 cm × 3.0 cm). Data were collected from at least three separate samples.

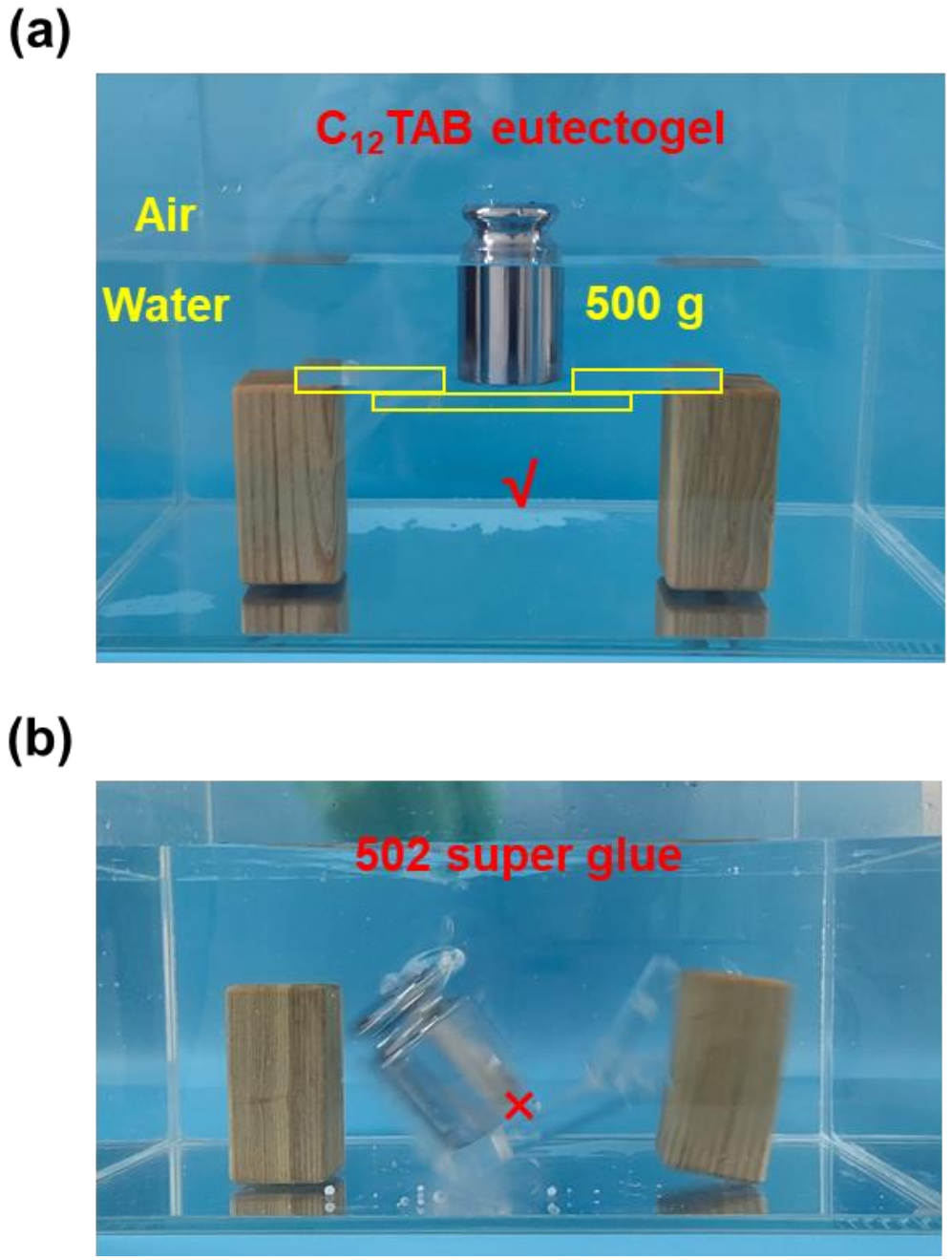

Figure S22. Underwater adhesiveness of 25.0 wt% C_{12}TAB/ChCl-urea eutectogel and representative commercial adhesives. Experimental site photos of (a) C_{12}TAB/ChCl-urea eutectogel and (b) 502 super glue (a cyanoacrylate adhesive).

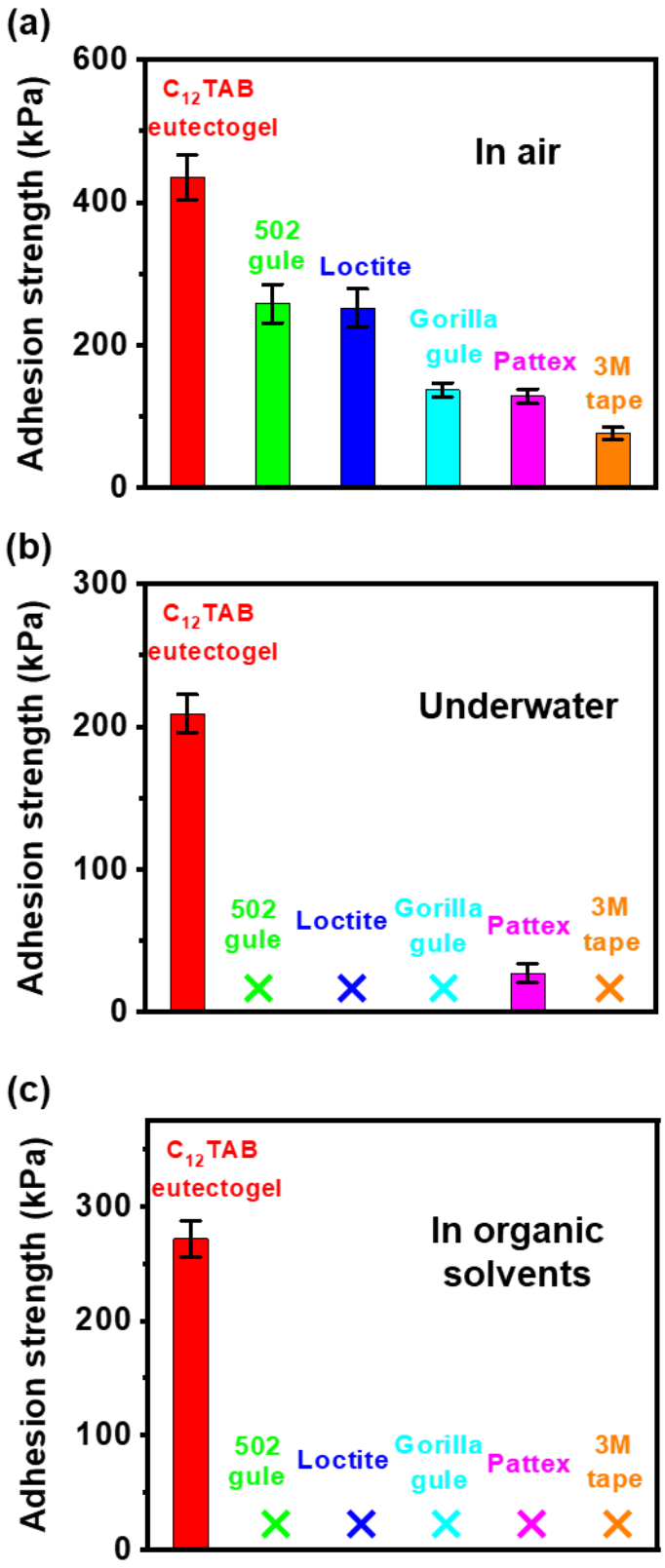

Figure S23. Comparison of the adhesion strength of the C_{12}TAB/ChCl-urea eutectogel and commercial adhesives on glass (a) in air, (b) underwater and (c) in organic solvents.

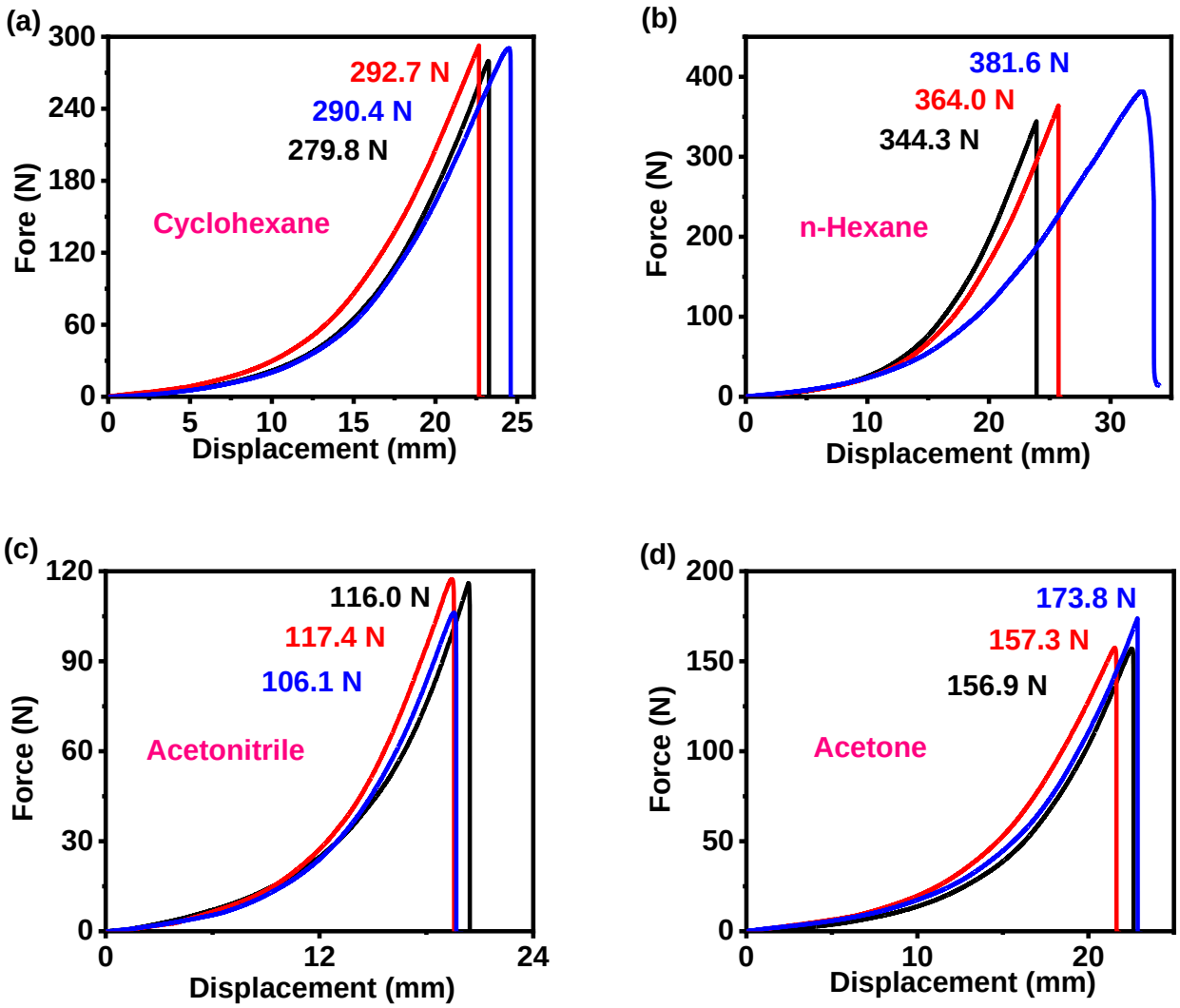

Figure S24. Lap-shear test curve of 25.0 wt% C_{12}TAB/ChCl-urea eutectogel adhered glass. The samples were *in situ* prepared in organic solvents by pressing ~5 min. Data were collected from at least three separate samples.

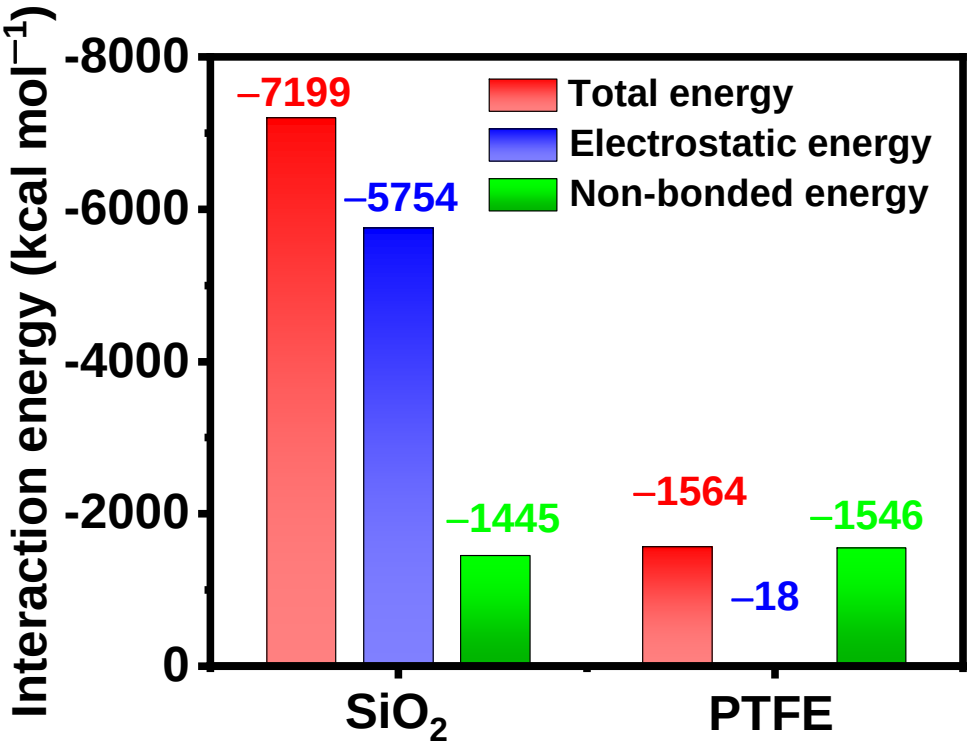

Figure S25. The interfacial binding energies between C_{12}TAB/ChCl-urea eutectogels and SiO_2 or PTFE substrates.

Table S2. Comparison for adhesion performance with previously reported low-molecular-weight supramolecular adhesives.

Material	Adhesion strength in air at RT		Ultra-low temperature adhesiveness	Underwater *in situ* adhesiveness	Organic solvent *in situ* adhesiveness	Long-term adhesiveness at RT	Ref
	Hydrophilic substrates	Hydrophobic substrates					
C_{12}TAB/ChCl-urea supramolecular eutectogel	**Glass (435.1 kPa)** **Fe (565.3 kPa)**	**PTFE (76.3 kPa)** **PMMA (173.7 kPa)**	**–196 °C (Glass: 299.2 kPa)** **–80 °C (Glass: 632.5 kPa)**	**Glass (209.9 kPa)**	**Cyclohexane (Glass: 479.4 kPa)** **n-Hexane (Glass: 605.5 kPa)**	**>15 days**	**This work**
Pt-coordinated benzo-21-crown-7-functionalized pyridine	Glass (273 psi)	PTFE (28 psi)	–20 °C (< 125 psi)	NA	NA	NA	14
Azobenzene derivatives	Al (1.34 MPa)	NA	NA	NA	NA	NA	15
Triply benzo-21-crown-7–substituted 1,3,5 benzenetricarboxamide derivative ($TC7_{10}$-H_1)	Glass (602 psi)	NA	–20 °C (293 psi)	NA	NA	More than two and a half years	16
L-histidine/$H_4SiW_{12}O_{40}$ (His/SiW)	Glass (15.8 kPa) Cu (38.3 kPa)	PET (356.4 kPa)	NA	NA	NA	NA	17
3-(2-naphthyl)-L-alanine and $H_6P_2W_{18}O_{62}$ (NA/HP_2W_{18})	NA	NA	NA	Glass (3.78 kPa) Stainless steel (4.33 kPa)	NA	NA	18

Continued

Material	Adhesion strength in air at RT		Ultra-low temperature adhesiveness	Underwater *in situ* adhesiveness	Organic solvent *in situ* adhesiveness	Long-term adhesiveness at RT	Ref
	Hydrophilic substrates	Hydrophobic substrates					
Cyclodextrin-acid-based DESPs	Glass (4.38 MPa) Fe (6.57 MPa)	PTFE (0.48 MPa) PMMA (1.68 MPa)	–80 °C (PMMA: 1.30 MPa)	NA	Dichloromethane[a] (Glass: 2.84 MPa)	over 90 days	19
Penta-Substituted cyanostar macrocycle/diphosphate monomer	Glass (1.6 MPa)	NA	NA	NA	NA	NA	20
Pillar[5]arene-crown ether (PC)-water copolymer (PC_{10}-W_1)	Glass (4.01 MPa) Steel (4.28 MPa)	PTFE (0.09 MPa) PMMA (0.46 MPa)	–80 °C (Steel: 1.25 MPa) –196 °C (Steel: 1.17 MPa)	NA	NA	90 days at −50 °C	21
Arylazoisoxazoles derivatives	Glass (bearing 0.840 kg load) Al (bearing 3.7 kg load)	Teflon (bearing 1.1 kg load) PMMA (bearing 3.8 kg load)	NA	NA	NA	3 days	22
Crown ether-Pt supramolecule (CPS)	Glass (1.52 MPa) Al (1.43 MPa)	NA	NA	NA	NA	180 days	23
Dibenzo-24-crown-8 with four-armed pentaerythritol (P1)	Glass (2.017 MPa) Wood (1.698 MPa)	PTFE (0.277 MPa) PMMA (0.790 MPa)	–18 °C (Wood: 0.967 MPa)	Glass (1.562 MPa) Wood (0.046 MPa)	NA	> 24 months	24

a: Organic solvent resistant adhesiveness, not *in situ* adhesiveness.

Section S4 References

[1] R. Gaussian, G. Trucks, H. Schlegel, G. Scuseria, M. Robb, J. Cheeseman, G. Scalmani, V. Barone, B. Mennuci, G. Petersson, H. Nakatsuji, M. Caricato, X. Li, H. Hratchian, A. Izmaylov, J. Bloino, G. Zheng, J. Sonnenberg, M. Hada, D. Fox, *Gaussian, Inc., Wallingford CT* **2009**.

[2] a) K. Raghavachari, *Theor. Chem. Acc.* **2000**, *103*, 361-363; b) M. Parrinello, A. Rahman, *Phys. Rev. Lett.* **1980**, *45*, 1196-1199; c) A. D. Becke, *J. Chem. Phys.* **1993**, *98*, 1372-1377; d) A. D. Becke, *J. Chem. Phys.* **1993**, *98*, 5648-5652.

[3] T. Lu, F. Chen, *J. Comput. Chem.* **2012**, *33*, 580-592.

[4] C. I. Bayly, P. Cieplak, W. Cornell, P. A. Kollman, *J. Phys. Chem.* **1993**, *97*, 10269-10280.

[5] H. J. C. Berendsen, D. van der Spoel, R. van Drunen, *Comput. Phys. Commun.* **1995**, *91*, 43-56.

[6] J. Wang, R. M. Wolf, J. W. Caldwell, P. A. Kollman, D. A. Case, *J. Comput. Chem.* **2004**, *25*, 1157-1174.

[7] L. Martínez, R. Andrade, E. G. Birgin, J. M. Martínez, *J. Comput. Chem.* **2009**, *30*, 2157-2164.

[8] G. Bussi, D. Donadio, M. Parrinello, *J. Chem. Phys.* **2007**, *126*, 014101.

[9] H. J. C. Berendsen, J. P. M. Postma, W. F. van Gunsteren, A. DiNola, J. R. Haak, *J. Chem. Phys.* **1984**, *81*, 3684-3690.

[10] C. Lee, W. Yang, R. G. Parr, *Phys. Rev. B* **1988**, *37*, 785-789.

[11] T. Darden, D. York, L. Pedersen, *J. Chem. Phys.* **1993**, *98*, 10089-10092.

[12] I. J. Chen, D. Yin, A. D. MacKerell Jr, *J. Comput. Chem.* **2002**, *23*, 199-213.

[13] F. S. Emami, V. Puddu, R. J. Berry, V. Varshney, S. V. Patwardhan, C. C. Perry, H. Heinz, *Chem. Mater.* **2014**, *26*, 2647-2658.

[14] Q. Zhang, T. Li, A. Duan, S. Dong, W. Zhao, P. J. Stang, *J. Am. Chem. Soc.* **2019**, *141*, 8058-8063.

[15] Z. Wu, C. Ji, X. Zhao, Y. Han, K. Muellen, K. Pan, M. Yin, *J. Am. Chem. Soc.* **2019**, *141*, 7385-7390.

[16] S. Dong, J. Leng, Y. Feng, M. Liu, C. J. Stackhouse, A. Schoenhals, L. Chiappisi, L. Gao, W. Chen, J. Shang, L. Jin, Z. Qi, C. A. Schalley, *Sci. Adv.* **2017**, *3,* eaao0900.

[17] J. Xu, X. Li, J. Li, X. Li, B. Li, Y. Wang, L. Wu, W. Li, *Angew. Chem. Int. Ed.* **2017**, *56*, 8731-8735; *Angew. Chem.* **2017**, *129,* 8857-8861.

[18] X. Li, Z. Du, Z. Song, B. Li, L. Wu, Q. Liu, H. Zhang, W. Li, *Adv. Funct. Mater.* **2018**, *28* ,1800599.

[19] S. Wu, C. Cai, F. Li, Z. Tan, S. Dong, *Angew. Chem. Int. Ed.* **2020**, *59*, 11871-11875; *Angew. Chem.* **2020**, *132,* 11969-11973.

[20] W. Zhao, J. Tropp, B. Qiao, M. Pink, J. D. Azoulay, A. H. Flood, *J. Am. Chem. Soc.* **2020**, *142*, 2579-2591.

[21] X. Li, J. Lai, Y. Deng, J. Song, G. Zhao, S. Dong, *J. Am. Chem. Soc.* **2020**, *142*, 21522-21529.

[22] L. Kortekaas, J. Simke, D. W. Kurka, B. J. Ravoo, *ACS Appl. Mater. Interfaces.* **2020**, *12*, 32054-32060.

[23] T. Li, Q. Zhang, D. Li, S. Dong, W. Zhao, P. J. Stang, *ACS Appl. Mater. Interfaces.* **2020**, *12*, 38700-38707.

[24] X. Li, Y. Deng, J. Lai, G. Zhao, S. Dong, *J. Am. Chem. Soc.* **2020**, *142*, 5371-5379.